Calcium atoms attached to mixed helium droplets: A probe for the ^{3}He-^{4}He interface

O. Bünermann,[1] M. Dvorak,[1] F. Stienkemeier,[1] A. Hernando,[2] R. Mayol,[2] M. Pi,[2] M. Barranco,[2] and F. Ancilotto[3]
[1]*Physikalisches Institut, Universität Freiburg, Hermann-Herder-Str. 3, D-76104 Freiburg, Germany*
[2]*Departament ECM, Facultat de Física, and IN2UB, Universitat de Barcelona, Diagonal 647, 08028 Barcelona, Spain*
[3]*Dipartimento di Fisica "G. Galilei," Università di Padova, via Marzolo 8, I-35131 Padova, Italy and CNR-INFM-DEMOCRITOS National Simulation Center, I-34014 Trieste, Italy*
(Received 22 April 2009; published 10 June 2009)

Experimental and theoretical results for mixed helium droplets doped with one calcium atom are reported. The absorption spectrum around the $4s4p \leftarrow 4s^2$ transition is calculated as a function of the composition of the droplet and compared to the experiment. Our study reveals the distinct feature that for specific ^{3}He concentrations, Ca atoms sit at the ^{3}He-^{4}He interface. This particular property of Ca, likely not shared with any other atomic or molecular species but the heavier alkaline-earth atoms, might offer the possibility of using it to probe the ^{3}He-^{4}He interface of the droplet.

DOI: 10.1103/PhysRevB.79.214511 PACS number(s): 36.40.−c, 33.20.Kf, 71.15.Mb

I. INTRODUCTION

Helium nanodroplets have attracted considerable interest in recent years because of their unique properties (see, e.g., Ref. 1 and references therein). In particular, superfluid droplets made of ^{4}He atoms provide an ideal matrix for spectroscopic studies at temperatures of 380 mK.[2] Superfluidity is instrumental to allow even rotational resolved spectra of molecules solvated in ^{4}He droplets.[3] Droplets made of ^{3}He atoms are colder (150 mK), but normal fluid;[4] the possibility to compare both systems gives valuable insight into the quantum nature of Bose and Fermi drops.[5]

Electronic spectroscopy is a powerful tool to reveal the structure of embedded impurities, the key observables to determine the position of an atomic impurity being the shift and width of the electronic transitions. Whereas almost all impurities are solvated inside helium droplets, alkali atoms are an exception. Irrespective of the isotope, they are weakly bound to helium droplets and reside in dimples on the drop surface.[6,7] The situation for alkaline-earth atoms is borderline; the heavier ones but magnesium reside in a deep dimple on the surface of ^{4}He droplets[8–10]—the case of Mg is still debated,[11] although it is most likely in a very delocalized state within the bulk of the droplet[12]—whereas experiments and recent calculations on ^{3}He drops have shown that alkaline-earth atoms reside in their bulk.[9]

Mixed ^{3}He-^{4}He droplets have also been produced and studied.[3,13–15] Because ^{3}He has a limited solubility in ^{4}He, these droplets have a core made of ^{4}He and a surrounding ^{3}He shell. The different solvation behavior of Ca and heavier alkaline-earth atoms in ^{3}He and ^{4}He drops might offer the unique possibility of using them to study the ^{3}He-^{4}He interface. The rationale of this statement is that Ca, Sr, and Ba impurities would dive into the fermionic shell up to reaching the surface of the ^{4}He core if the appropriate number of atoms of each isotope is chosen. This paper reports on experiments and calculations that confirm this guess for calcium atoms, the limiting case.

II. METHODS AND RESULTS

Our theoretical analysis is carried out within density-functional theory,[16] using the Ca-He $X^1\Sigma$ potential of Ref. 17 for the ground state, and the $^1\Pi$ and $^1\Sigma$ potentials of Ref. 10 for the excited states. The energy of the Ca-helium system is written as a functional of the Ca wave function $\Phi(\mathbf{r})$, the ^{4}He order parameter $\Psi(\mathbf{r})=\sqrt{\rho_4(\mathbf{r})}$, where $\rho_4(\mathbf{r})$ is the ^{4}He atomic density normalized to N_4 atoms, and the ^{3}He particle and kinetic-energy densities $\rho_3(\mathbf{r})$ and $\tau_3(\mathbf{r})$. To handle the large number of ^{3}He atoms N_3 involved in current experiments, we have used a Thomas-Fermi approximation to express $\tau_3(\mathbf{r})$ as a function of $\rho_3(\mathbf{r})$ and its gradient.[7] Within the pair-potential approximation, we write the energy of the system as[10,16]

$$E[\Psi,\Phi,\rho_3,\tau_3]=\frac{\hbar^2}{2m_{^4\mathrm{He}}}\int d\mathbf{r}|\nabla\Psi(\mathbf{r})|^2+\int d\mathbf{r}\mathcal{E}(\rho_4,\rho_3,\tau_3)+\frac{\hbar^2}{2m_{Ca}}\int d\mathbf{r}|\nabla\Phi(\mathbf{r})|^2+\int\int d\mathbf{r}d\mathbf{r}'|\Phi(\mathbf{r})|^2V_{X^1\Sigma}(|\mathbf{r}-\mathbf{r}'|)\rho_{3+4}(\mathbf{r}'). \quad (1)$$

We have self-consistently solved the equations that result from the variations in Eq. (1) with respect to Ψ, Φ, and $\rho_3(\mathbf{r})$ (see Ref. 10 for the details).

Figure 1 shows the ^{3}He equidensity lines for several Ca@^{4}He$_{1000}$+^{3}He$_{N_3}$ droplets. It can be seen how the Ca atom is progressively immersed into the droplet as N_3 increases, and how the dimple at the ^{3}He-^{4}He interface is progressively flattening out. It is worth recalling that the ^{3}He shell is at fairly low density until N_3 is larger than a few thousands.[18] Thus, an apparently full-coated impurity might not yield the bulk liquid ^{3}He shift.

Another view of the doped droplet is presented in Fig. 2, where we show the Ca@^{4}He$_{1000}$+^{3}He$_{2000}$ structure. One cut displays the undoped ^{3}He-^{4}He interface, whereas the other cut displays the interface distorted by the presence of the Ca bubble. These results show that Ca indeed resides in a bubble close to the interface.

Once the helium densities and impurity wave function have been determined as outlined before, to obtain the absorption spectrum around the $4s4p \leftarrow 4s^2$ transition we have

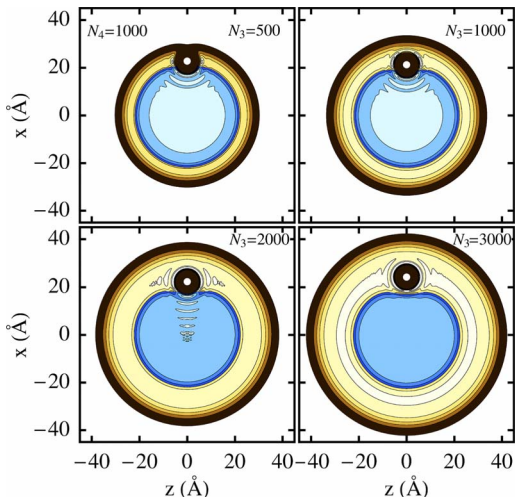

FIG. 1. (Color online) Helium density distribution on the $y=0$ plane of symmetry for $N_4=1000$ and the indicated N_3 values. The white dot is at the point where the Ca probability density has its maximum value. For each isotope, we have plotted several equidensity lines between those corresponding to 0.2 to $1.4\times\rho_b$, in 0.2 $\times\rho_b$ steps, where ρ_b is the bulk liquid density, $\sim$0.0163 Å^{-3} for ^{3}He and $\sim$0.0218 Å^{-3} for ^{4}He. In the overlapping region, only the contours corresponding to the maximum $\{\rho_3,\rho_4\}$ are shown.

resorted to an atomiclike simulation inspired by that proposed in Ref. 19, where the helium density is stochastically represented by a large number of hard spheres configurations. For each configuration, a set of N_4+N_3 positions $\{\mathbf{r}_i\}$ is randomly generated by importance sampling techniques[20] using $\rho_4(\mathbf{r})/N_4$ and $\rho_3(\mathbf{r})/N_3$ as probability density functions, respectively. The diameter of the hard spheres is set to the coarse-grained core radius value used in the energy functional.[16] The position of the impurity $\mathbf{r}_{Ca}$ is randomly generated using $|\Phi|^2$ as probability density, and the excitation energy is computed as the difference between the eigenvalues of the excited-state energy matrix $\Sigma_i U(\mathbf{r}_i-\mathbf{r}_{Ca})$ [Eq. (16) of Ref. 10], and the pairwise sum of the ground-state pair-potential interactions $\Sigma_i V_{X^1\Sigma}(|\mathbf{r}_i-\mathbf{r}_{Ca}|)$. The absorption

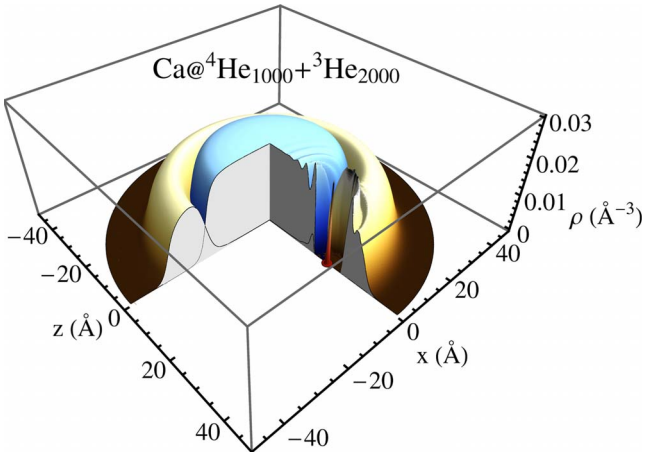

FIG. 2. (Color online) Three-dimensional view of the Ca@^{4}He$_{1000}$+^{3}He$_{2000}$ droplet. Also shown is the probability density of Ca in arbitrary units.

spectrum is just the excitation energy histogram obtained by repeating this procedure for all configurations, and will be discussed below.

Along with the calculations, we have carried out experiments in a helium droplet machine used before for electronic spectroscopy studies.[7,8] We recall that pressurized very cold helium gas is expanded through a small nozzle (5 μm) into vacuum. Droplets are formed by condensation. Downstream, the droplets are doped in an oven via the pick-up technique and finally crossed with the beam of a pulsed dye laser. The laser-induced fluorescence is collected by a lens system and recorded in a photomultiplier tube. Mixed droplets are formed by coexpansion of ^{3}He-^{4}He gas mixtures at 20 bars and 10–15 K, depending on the composition. To achieve a substantial proportion of ^{3}He in the droplets, gas mixtures with high ^{3}He concentrations $x_3=N_3/(N_4+N_3)$ were required. The reason is that ^{3}He atoms have a binding energy about three times smaller than ^{4}He atoms. This lower binding energy hampers condensation into clusters (^{3}He clusters are energetically stable only at sizes $N_3\gtrsim 30$.[21]) Moreover, ^{3}He atoms reside in the droplet outer shell. Hence, mostly ^{3}He evaporates in the droplet cooling process. Determining the actual size of the droplet is not straightforward for droplets produced in a coexpansion jet. Since at the chosen conditions pure droplets of both isotopes are of comparable mean size N, we are somewhat confident that under these conditions also the mixed droplets have a size of $N=N_3+N_4\sim 5000$.

To determine the composition of the formed mixtures, droplets are ionized via electron impact and the fragment ions are detected with a quadrupole mass spectrometer. The ratio of detected ions, ^{3}He$^+$/^{4}He$^+$, is used to determine the ^{3}He concentration before doping. Upon doping, the ^{3}He concentration changes because the energy deposited into the droplet by the capture of a Ca atom ($\sim$1400 cm^{-1}) is essentially dissipated by the evaporation of ^{3}He only. In a thermodynamic picture, the number of evaporated ^{3}He atoms is estimated to be $\sim$850, as the binding energy of ^{3}He is about 1.7 cm^{-1}.

We have recorded the absorption spectrum of the $4s4p \leftarrow 4s^2$ transition of calcium bound to mixed droplets as a function of x_3. Let us first focus on the absorption of Ca bound to pure ^{3}He and ^{4}He droplets ($x_3=100$, $x_3=0$). Experimentally—see Fig. 3—the shift for ^{3}He is larger than for ^{4}He and perfectly matches that of Ca in bulk ^{3}He.[22] This confirms the interpretation, based on previous measurements for Sr as well as theoretical predictions for Ca,[9,23] that calcium is solvated inside ^{3}He droplets. We also show in Fig. 3 the computed spectra for Ca in liquid ^{3}He and ^{4}He, and in a ^{4}He$_{2000}$ droplet. The line shape is well reproduced by the calculations. However, for bulk liquids, the calculations underestimate the experimental results[22] by some 25 cm^{-1}. We attribute this disagreement to some inaccuracy in the excited Ca-He potentials we have used.

Figures 4 and 5 show the experimental as well as calculated shifts and widths, respectively, as a function of x_3. To understand the apparently larger disagreement between theory and experiment for pure ^{4}He droplets ($x_3=0$), one has to note that in Fig. 5 the total number of atoms in the droplet is not kept constant as in Fig. 4 but falls well below N

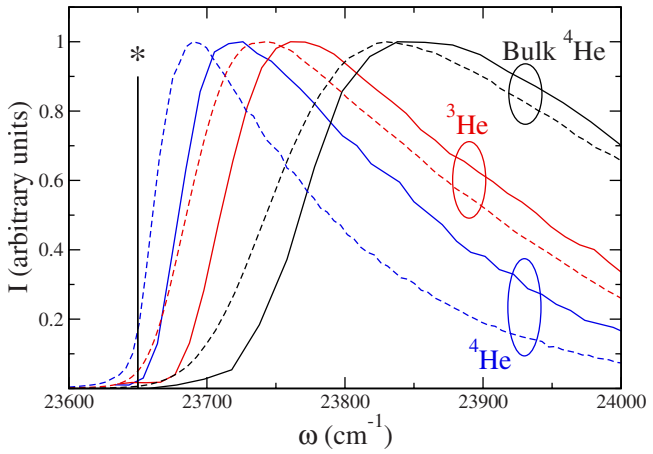

FIG. 3. (Color online) Spectrum of Ca bound to pure ^{3}He and ^{4}He droplets made of ~5000 helium atoms and of liquid ^{4}He (Ref. 22) around the $4s4p \leftarrow 4s^2$ transition (solid lines). Also shown are the computed spectra for Ca in bulk liquid and in a $^4He_{2000}$ droplet (dashed lines). The vertical line indicates the unshifted transition.

=2000 for $x_3 < 20$. It has been experimentally shown[8] that for these small droplets the shift drastically falls. In this way, the corresponding calculated values have to be lower in comparison to the experimental data and bulk helium values.

The measured shifts for mixed droplets are close to the pure ^{4}He droplet value if x_3 is below 70%. At higher ^{3}He concentrations, the shift suddenly rises and overshoots the pure ^{3}He droplet value. Above $x_3 \sim 80\%$, the measured shift is similar to that of pure ^{3}He drops. The width of the spectrum displays a similar behavior, with a stepwise change arising at $x_3 \sim 80\%$ to reach the ^{3}He value. The behavior for large concentrations, and in particular the amount of overshooting, is nicely reproduced by the calculations. The calculated stepwise behavior is not so pronounced. However, keeping in mind the systematic deviation to lower values for concentrations somewhat below $x_3 \lesssim 45\%$, the agreement is quite satisfactory.

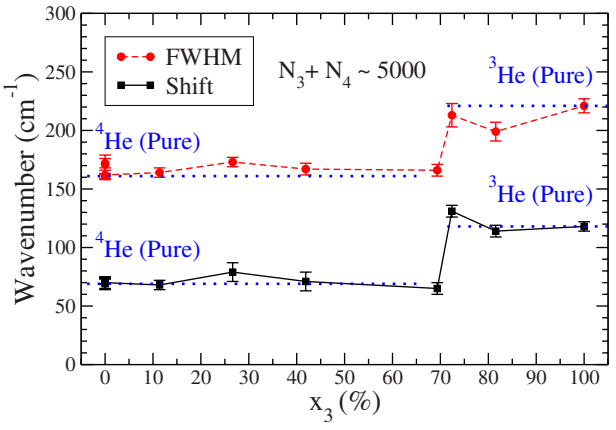

FIG. 4. (Color online) Measured shift and full width at half maximum (FWHM) in cm^{-1} as a function of the ^{3}He concentration. Also indicated by dotted lines are the experimental values for a $^3He_{5000}$ droplet (118 cm^{-1} shift and 221 cm^{-1} width) and for a $^4He_{5000}$ droplet (71 cm^{-1} shift and 161 cm^{-1} width). The lines have been drawn as a guide to the eye.

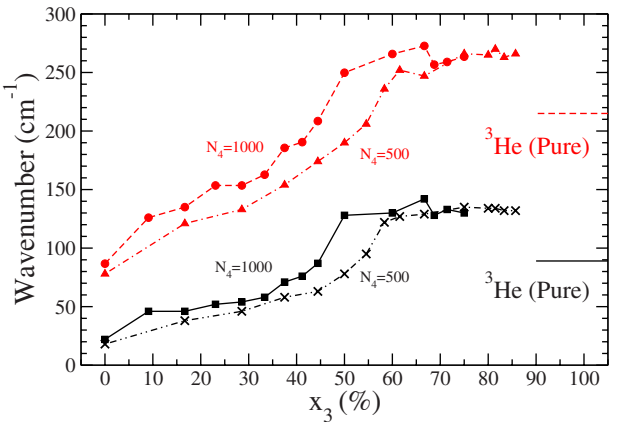

FIG. 5. (Color online) Calculated shift (lower two curves) and FWHM (upper two curves) in cm^{-1} as a function of the ^{3}He concentration for N_4=500 and 1000, and different N_3 values. From left to right, the symbols correspond to N_3=0, 100, 200, 300, 400, 500, 600, 700, 800, 1000, 1500, 2000, 2200, 2500, and 3000. Also shown are the values obtained for bulk liquid ^{3}He. The lines have been drawn as a guide to the eye.

The sizeable increase in the calculated shift at fixed N_4 and low x_3 is expected due to the tendency of the lighter isotope to surround the impurity. This increase is followed by a x_3 range up to ~35% in which the shift is little sensitive to the drop composition. We attribute this insensitivity to the compensation of two effects: the shift increases as the coating by ^{3}He atoms increases, but it decreases as the Ca atom is progressively detached from the interface. The sizeable rising coincides with the full coating onset of the impurity in the outer ^{3}He shell (see Fig. 1). The rigid $x_3 \sim 8\%$ displacement between the N_4=500 and 1000 shifts can be understood using a sharp density model for the helium densities. We mention that the wiggles in the shift and width arise from the structure of the solvation shells already found, e.g., for Mg impurities.[12]

Since the shift roughly depends on the total helium density around the Ca bubble, a value larger than that of liquid ^{3}He is a clear indication that the impurity is attached to the interface, where it partly feels the denser ^{4}He environment. Eventually, the ^{3}He shell is so thick that Ca detaches from the interface and sits in a nearly pure ^{3}He environment, the shift becoming that of liquid ^{3}He. The appearance of the detached state is illustrated in Fig. 6, where we display the density profile of a mixed helium slab, which we use to mimic a mixed drop with a very large amount of both helium isotopes. Thus, the shift overshooting is a clear signature of the interface location of the Ca impurity and the gradual evolution of the shift toward the bulk ^{3}He value, a signature of its detaching.

We have no conclusive explanation for the nearly constant shift and width experimentally found up to $x_3 \sim 70\%$. One possible justification is that the decrease in these observables as N_4 decreases[8] is compensated by a similar increasing due to the growing in N_3 so as to roughly have the same N for all the experimental droplets.

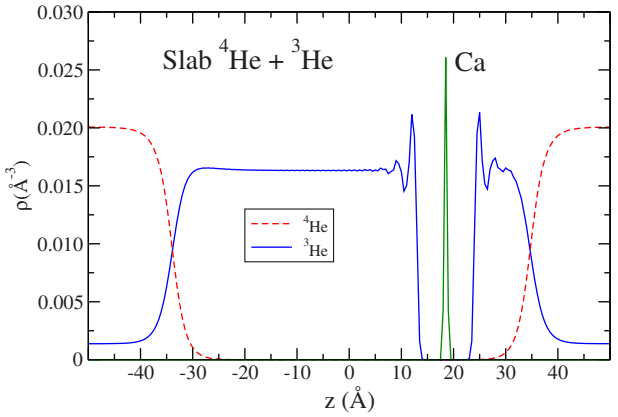

FIG. 6. (Color online) Density profile for the Ca@^{4}He-^{3}He interface in a slab geometry. Also shown is the probability density of Ca in arbitrary units.

III. SUMMARY AND OUTLOOK

We have experimentally found that Ca atoms completely solvate inside ^{3}He droplets, and that for specific mixed helium drops, they reside in bubbles at or near the ^{3}He-^{4}He interface. This scenario has been confirmed by density-functional calculations. Consequently, a gentle perturbation of the Ca bubble might likely excite a sound wave at the interface, thus making accessible its study. Conversely, interfacial excitations would be affected by the presence of the Ca bubble, thus allowing to further probe its structure. Obtaining and/or detecting the excited modes of a mixed helium droplet is far from trivial, even in the case of undoped droplets. Theoretically, this can be addressed within the small amplitude limit of time-dependent density-functional theory; we refer the interested reader to Ref. 14 and references therein for a discussion of the properties of these modes in the case of drops made of either isotope.

Mixed droplets doped with alkali atoms when N_3 is fairly small as compared with N_4 are also worth to be studied. In particular, the atomic shift would provide information on the structure of the tiny ^{3}He shell around the ^{4}He core.

Finally, the study of bulk liquid isotopic mixtures doped either with simple atomic impurities or electrons, which can be carried out under well-controlled conditions of pressure and composition, may help shed light on the origin of the mentioned differences between experimental and calculated spectra on the one hand, and on the structure of the atom or electron bubble in helium mixtures on the other hand. This has interesting implications for the study of cavitation in liquid-helium mixtures.[24,25] Work along these lines is in progress.

ACKNOWLEDGMENTS

We thank Ll. Brualla, J. M. Fernández, D. Mateo, and F. Salvat for useful discussions. This work has been performed in part under Grant No. FIS2008–00421/FIS from DGI, Spain (FEDER).

[1] J. P. Toennies and A. F. Vilesov, Angew. Chem., Int. Ed. **43**, 2622 (2004); F. Stienkemeier and K. K. Lehmann, J. Phys. B **39**, R127 (2006); J. Tiggesbäumker and F. Stienkemeier, Phys. Chem. Chem. Phys. **9**, 4748 (2007); M. Y. Choi, G. E. Douberly, T. M. Falconer, W. K. Lewis, C. M. Lindsay, J. M. Merrit, P. L. Stiles, and R. E. Miller, Int. Rev. Phys. Chem. **25**, 15 (2006); K. Szalewicz, *ibid.* **27**, 273 (2008).

[2] R. Fröchtenicht, J. P. Toennies, and A. Vilesov, Chem. Phys. Lett. **229**, 1 (1994); M. Hartmann, R. E. Miller, J. P. Toennies, and A. Vilesov, Phys. Rev. Lett. **75**, 1566 (1995).

[3] S. Grebenev, J. P. Toennies, and A. F. Vilesov, Science **279**, 2083 (1998).

[4] J. Harms, M. Hartmann, J. P. Toennies, A. F. Vilesov, and B. Sartakov, J. Mol. Spectrosc. **185**, 204 (1997).

[5] M. Hartmann, F. Mielke, J. P. Toennies, A. F. Vilesov, and G. Benedek, Phys. Rev. Lett. **76**, 4560 (1996).

[6] F. Ancilotto, E. Cheng, M. W. Cole, and F. Toigo, Z. Phys. B: Condens. Matter **98**, 323 (1995); F. Stienkemeier, J. Higgins, C. Callegari, S. I. Kanorsky, W. E. Ernst, and G. Scoles, Z. Phys. D: At., Mol. Clusters **38**, 253 (1996); F. R. Brühl, R. A. Trasca, and W. E. Ernst, J. Chem. Phys. **115**, 10220 (2001); O. Bünermann, M. Mudrich, M. Weidemüller, and F. Stienkemeier, *ibid.* **121**, 8880 (2004).

[7] F. Stienkemeier, O. Bünermann, R. Mayol, F. Ancilotto, M. Barranco, and M. Pi, Phys. Rev. B **70**, 214509 (2004); R. Mayol, F. Ancilotto, M. Barranco, M. Pi, O. Bünermann, and F. Stienkemeier, J. Low Temp. Phys. **138**, 229 (2005); O. Bünermann, G. Droppelmann, A. Hernando, R. Mayol, and F. Stienkemeier, J. Phys. Chem. A **111**, 12684 (2007).

[8] F. Stienkemeier, F. Meier, and H. O. Lutz, J. Chem. Phys. **107**, 10816 (1997); Eur. Phys. J. D **9**, 313 (1999).

[9] A. Hernando, R. Mayol, M. Pi, M. Barranco, F. Ancilotto, O. Bünermann, and F. Stienkemeier, J. Phys. Chem. A **111**, 7303 (2007).

[10] A. Hernando, M. Barranco, R. Mayol, M. Pi, and M. Krośnicki, Phys. Rev. B **77**, 024513 (2008).

[11] J. Reho, U. Merker, M. R. Radcliff, K. K. Lehmann, and G. Scoles, J. Chem. Phys. **112**, 8409 (2000); Y. Ren and V. V. Kresin, Phys. Rev. A **76**, 043204 (2007); A. Przystawik, S. Göde, T. Döppner, J. Tiggesbäumker, and K.-H. Meiwes-Broer, *ibid.* **78**, 021202(R) (2008).

[12] A. Hernando, M. Barranco, R. Mayol, M. Pi, and F. Ancilotto, Phys. Rev. B **78**, 184515 (2008).

[13] J. Harms, M. Hartmann, B. Sartakov, and J. P. Toennies, J. Chem. Phys. **110**, 5124 (1999); S. Grebenev, E. Lugovoi, B. G. Sartakov, J. P. Toennies, and A. F. Vilesov, Faraday Discuss. **118**, 19 (2001).

[14] M. Barranco, R. Guardiola, S. Hernández, R. Mayol, and M. Pi, J. Low Temp. Phys. **142**, 1 (2006).

[15] S. Fantoni, R. Guardiola, J. Navarro, and A. Zucker, J. Chem. Phys. **123**, 054503 (2005); D. Bressanini and G. Morosi, Phys. Rev. Lett. **90**, 133401 (2003); D. Mateo, M. Barranco, R. Mayol, J. Navarro, and M. Pi, Eur. Phys. J. D **52**, 63 (2009).

[16] M. Barranco, M. Pi, S. M. Gatica, E. S. Hernández, and

J. Navarro, Phys. Rev. B **56**, 8997 (1997).
[17] R. J. Hinde, J. Phys. B **36**, 3119 (2003).
[18] M. Pi, R. Mayol, and M. Barranco, Phys. Rev. Lett. **82**, 3093 (1999).
[19] T. Nakatsukasa, K. Yabana, and G. F. Bertsch, Phys. Rev. A **65**, 032512 (2002).
[20] F. Salvat, J. M. Fernández, and J. Senpau, *Penelope-2008: A Code System for Monte Carlo Simulation of Coupled Electron-Photon Transport* (OECD Nuclear Energy Agency, Issy-les-Moulineaux, France, 2009) http://www.nea.fr/html/dbprog/peneloperef.html.
[21] M. Barranco, J. Navarro, and A. Poves, Phys. Rev. Lett. **78**, 4729 (1997); R. Guardiola and J. Navarro, Phys. Rev. A **71**, 035201 (2005); E. Sola, J. Casulleras, and J. Boronat, Phys. Rev. B **73**, 092515 (2006).
[22] Y. Moriwaki and N. Morita, Eur. Phys. J. D **33**, 323 (2005).
[23] J. Navarro and R. Guardiola (unpublished).
[24] M. Barranco, M. Guilleumas, M. Pi, and D. M. Jezek, in *Microscopic Approaches to Quantum Liquids in Confined Geometries*, edited by E. Krotscheck and J. Navarro (World Scientific, Singapore, 2002).
[25] H. J. Maris, J. Phys. Soc. Jpn. **77**, 111008 (2008).